Mathematical Geology, Vol. 30, No. 6, 1998

Automatic Modeling of (Cross) Covariance Tables Using Fast Fourier Transform[1]

Tingting Yao[2] and Andre G. Journel[2]

Covariance models provide the basic measure of spatial continuity in geostatistics. Traditionally, a closed-form analytical model is fitted to allow for interpolation of sample covariance values while ensuring the positive definiteness condition. For cokriging, the modeling task is made even more difficult because of the restriction imposed by the linear coregionalization model. Bochner's theorem maps the positive definite constraints into much simpler constraints on the Fourier transform of the covariance, that is the density spectrum. Accordingly, we propose to transform the experimental (cross) covariance tables into quasidensity spectrum tables using Fast Fourier Transform (FFT). These quasidensity spectrum tables are then smoothed under constraints of positivity and unit sum. A backtransform (FFT) yields permissible (jointly) positive definite (cross) covariance tables. At no point is any analytical modeling called for and the algorithm is not restricted by the linear coregionalization model. A case study shows the proposed covariance modeling to be easier and much faster than the traditional analytical covariance modeling, yet yields comparable kriging or simulation results.

KEY WORDS: covariance models, Bochner's theorem, fast Fourier transform.

INTRODUCTION

Covariance models provide the basic measure of spatial continuity of a random field. A permissible positive definite model is required to interpolate sample covariance values toward uninformed distance vectors. The positive definiteness property ensures existence and uniqueness of solutions to the kriging systems. The traditional modeling approach considers only positive linear combination of basic models known to be positive definite. The restriction to linear combinations is sometimes limitative and the modeling process can be time-demanding and is somewhat subjective. For cokriging the modeling of a cross-covariance matrix between primary and secondary variable(s) is even more difficult because of further restrictions imposed by the linear coregionalization model (Journel and Huijbregts, 1978; Goulard, 1989).

[1]Received 29 April 1997; accepted 1 October 1997.

[2]Department of Geological & Environmental Sciences, Stanford University, Stanford, California 94305. e-mail: tingting@pangea.stanford.edu

0882-8121/98/0800-0589$15.00/1

A nonparametric alternative to analytical covariance modeling would be based on Bochner's theorem (1949). The theorem states that a function $C(\mathbf{h})$ is positive definite if and only if it can be expressed as the Fourier transform of a bounded nondecreasing positive measure $S(\mathbf{w})$:

$$C(\mathbf{h}) = \int_{\Re^d} e^{2\pi i \mathbf{h} \cdot \mathbf{w}} \, dS(\mathbf{w}) \tag{1}$$

where $\mathbf{h}$ is the distance vector in the d- dimension space $\Re^d$ and $\mathbf{w}$ is the frequency vector in the corresponding frequency domain.

If the stationary random function (RF) model $Z(\mathbf{u})$ has unit variance, i.e., $C(\mathbf{0}) = \text{Var}\{Z(\mathbf{u})\} = 1$, then $S(\mathbf{w})$ can be seen as a cumulative distribution function (*cdf*), with $dS(\mathbf{w}) = s(\mathbf{w})\, d\mathbf{w}$. Bochner's theorem then requires that the density $s(\mathbf{w}) = dS(\mathbf{w})/d\mathbf{w}$ be a probability density function (*pdf*), i.e., such that:

$$s(\mathbf{w}) \geq 0, \ \forall \mathbf{w}$$

$$\int_{\Re^d} s(\mathbf{w}) \, d\mathbf{w} = 1 \tag{2}$$

$s(\mathbf{w})$ is called the spectral density or density spectrum of RF $Z(\mathbf{u})$.

The previous integral can be approximated by the discrete sum:

$$C(\mathbf{h}) = \sum_{k=1}^{K} e^{2\pi i \mathbf{h} \mathbf{w}} \, s(\mathbf{w}_k), \qquad k = 1, \ldots, K \tag{3}$$

In Rehman (1995), the series $s(\mathbf{w}_k)$ is determined by minimizing the weighted least-squared differences between sample covariance and model covariance values. For an isotropic model, that discrete sum can be replaced by *Bessel* or *sinc* functions (Sneddon, 1951):

in 2-D:

$$C(h) = \sum_{k=1}^{K} w J_0(wh) s(w) \, dw, \qquad h, w = \Re^1$$

where $J_0(\cdot)$ is the *Bessel* function of zero order, and $h = |\mathbf{h}|$, $w = |\mathbf{w}|$.

in 3-D:

$$C(h) = \sum_{k=1}^{K} w^2 \, \text{sinc}(wh) s(w) \, dw, \qquad h, w \in \Re^1$$

where $sinc(\cdot) = [\sin(\cdot)/\cdot]$ is the *sinc* function, and again $h = |\mathbf{h}|$, $w = |\mathbf{w}|$.

In the 3-D space $\Re^3$ under anisotropic conditions, Rehman's algorithm requires a large level of discretization (K^3 terms), which could lead to convergence problems. Using the traditional prior coordinate transformation (rotations

and affinity) to correct for anisotropy makes the optimization problem (3) nonlinear, rendering its solution even more complex.

In the line of Rehman's pioneering attempt, this research work aims at a complete automatic variogram/covariance modeling that does not call for any specific analytical model. The fundamental idea is still based on Bochner's theorem but does not require fitting a long series of spectral density values $s(\mathbf{w}_k)$ as in relation (3). The final result is a covariance lookup table for constructing the kriging systems during estimation or simulation. This covariance lookup table must be positive definite. The key to such automatic fitting lies in Fast Fourier Transform (*FFT*). A first *FFT* transforms the original experimental pseudo[3] covariance table or map into a quasidensity spectrum, a smoothing algorithm is then applied to get a licit density spectrum table. That density spectrum can be used directly to perform spectral simulation, or it can be inverse-transformed by *FFT* into a licit covariance lookup table for estimation or simulation in the spatial domain.

In addition to shortcutting the tedious and subjective task of fitting analytical (cross) covariance models, this "automatic *FFT* covariance modeling" has the potential for integration of related soft information such as structural geological or geophysical interpretation during the smoothing of either the sample covariance table or the quasispectrum table. Note that a smoothing process carried out in the spectral domain is particularly attuned to data defined in the frequency domain, such as seismic velocity.

FFT MODELING OF A COVARIANCE TABLE

The original sample covariance table is generally not positive definite, because each lag is calculated independently of the others using different data pairs (Journel, 1996). Were such sample covariance values used as is, singular kriging matrices or negative estimation variances may result. In addition, not all covariance values needed are experimentally available, hence the sample covariance values must be interpolated to fill up the covariance table needed. Again, such interpolation may only give a pseudocovariance table which does not fulfill the positive definiteness condition. Correction for that property is best done in the spectral domain building on Bochner's theorem.

With Fast Fourier Transform, a gridded and previously completed pseudocovariance map $C(\mathbf{h})$ can be transformed into a gridded pseudospectrum map $s(\mathbf{w})$. In 2-D, that spectrum map is defined by the integral transform:

$$s(\omega_1, \omega_2) = \frac{1}{4\pi^2} \int_{-\infty}^{+\infty} dh_1 \int_{-\infty}^{+\infty} C(h_1, h_2) \exp\left[-i(\omega_1 h_1 + \omega_2 h_2)\right] dh_2$$

[3]By "pseudo" covariance table, we mean a table that may not fulfill the positive definite condition. Similarly, a quasi-density spectrum table may not fulfill the condition (2).

Or, in discrete form:

$$s(j_1, j_2) = \sum_{k_1=0}^{N_1-1} \sum_{k_2=0}^{N_2-1} C(k_1, k_2) \exp\left[-2\pi i\left(\frac{k_1 j_1}{} + \frac{k_2 j_2}{}\right)\right],$$

$$j_1 = 0, \ldots, N_1 - 1, \quad j_2 = 0, \ldots, N_2 - 1 \qquad (4)$$

According to Bochner's theorem, the general form of a real-valued positive definite function $C(h_1, h_2)$, continuous at $\mathbf{h} = 0$, is:

$$C(h_1, h_2) = \int_{-\infty}^{+\infty} \int_{-\infty}^{+\infty} \cos\left(\omega_1 h_1 + \omega_2 h_2\right) \cdot dS(\omega_1, \omega_2)$$

where $dS(\omega_1, \omega_2)$ is a bounded positive measure.

Because the original sample covariance table is not positive definite, its experimental density spectrum table may not be licit either: resulting s-values can be less than 0 and sum up to a value different from 1. To ensure positivity of the 2-D table $s(\omega_1, \omega_2)$ and a unit sum, we can smooth the original s-values under these two constraints. Such smoothing also removes unwanted sample fluctuations. The result is now a licit spectral pdf. The *FFT* backtransform of that licit and smooth spectral pdf is then a positive definite and smooth covariance table.

The final covariance table is thus built from a "roundtrip" *FFT* plus intermediate smoothing process(es) rather than from a Fourier series approximation of the original covariance values as in relation (3). We expect our proposed algorithm to be faster yet more flexible and accurate (closer to the sample covariance values if so desired) than Rehman's algorithm.

Implementation of the modeling algorithm proposed is hereafter detailed with derivation explicited for a 2-D space.

Calculation of the Sample Covariance Map

From the available data, gridded or scattered, a discrete covariance map (Chu, 1993) can be calculated for the available lag distances. As for calculation of any sample covariance $\hat{C}(\mathbf{h})$, proper tolerance on the lag vector $\mathbf{h}$ should be considered to avoid estimating a value from too few pairs. Interpolation is then used to fill in uninformed or replace poorly informed original entries in the covariance table. The size and discretization of the covariance table after interpolation should be such to allow finding all covariance values needed by future kriging systems.

- Sample covariance map

The formula for calculating the autocovariance is:

$$C_Z(\mathbf{h}) = \frac{1}{N(\mathbf{h})} \sum_{\alpha=1}^{N(\mathbf{h})} z(\mathbf{u}_\alpha) \cdot z(\mathbf{u}_\alpha + \mathbf{h}) - m_{Z-\mathbf{h}} m_{Z+\mathbf{h}}$$

where $m_{Z_{-\mathbf{h}}}$ is the mean of the pair tail values and $m_{Z_{+\mathbf{h}}}$ is the mean of the pair head values. Recall that an autocovariance is symmetric in $\mathbf{h}$, $-\mathbf{h}$.

- Cross-covariance map

Similarly, the formula for calculating the cross-covariance are:

$$C_{ZY}(\mathbf{h}) = \frac{1}{N(\mathbf{h})} \sum_{\alpha=1}^{N(\mathbf{h})} z(\mathbf{u}_\alpha) \cdot y(\mathbf{u}_\alpha + \mathbf{h}) - m_{Z_{-\mathbf{h}}} m_{Y_{+\mathbf{h}}}$$

$$C_{YZ}(\mathbf{h}) = \frac{1}{N(\mathbf{h})} \sum_{\alpha=1}^{N(\mathbf{h})} y(\mathbf{u}_\alpha) \cdot z(\mathbf{u}_\alpha + \mathbf{h}) - m_{Y_{-\mathbf{h}}} m_{Z_{+\mathbf{h}}}$$

Note: $C_{ZY}(\mathbf{h}) \neq C_{ZY}(-\mathbf{h})$, however, $C_{ZY}(\mathbf{h}) = C_{YZ}(-\mathbf{h})$.

The *GSLIB* program **varmap** can be used to calculate such covariance map (Deutsch and Journel, 1997). Because of the limited number of data, the number of pairs used for some of the covariance map cells may be too small, thus introducing noise in that map. In this case, a tolerance, denoted (τ_x, τ_y) in 2-D, is applied such that, whenever a data pair occurs in a cell (x, y), it is considered to contribute also in all cells within its neighborhood $(x', y') \in \{x \pm \tau_x, y \pm \tau_y\}$. This tolerance allows the same data pair to contribute to many covariance cells (lags), thus increasing the total number of data pairs available for calculation of each sample covariance value and providing a preliminary smoothing (Chu, 1993).

Preliminary Smoothing of the Covariance Map

Due to data sparsity, there could still be large fluctuations and missing entries in the original sample covariance table, which must therefore be smoothed and completed before being transformed by *FFT*. The program **intpmap** allows one to fill in missing values while performing a smoothing of the original covariance map. For each entry, the smoothed value is a weighted average of original values within a moving window (see Fig. 1). The weight associated to each original value is proportional to the number of data pairs used to derive it and decreases with the distance of that value from the center of the window. For a covariance entry at row k_1 and column k_2 with polar coordinate (ρ, θ), the smoothing window is a fan with angle $\theta + \Delta\theta$ and radius $(1 \pm \omega)\rho$ (see Fig. 1). The smoothed covariance value is then:

$$C(k_1, k_2) = \sum_{i=1}^{N} \lambda_i C_i \tag{5}$$

where N is the total number of original entry values found within the smoothing window, C_i is the ith covariance value and λ_i is the corresponding weight defined as:

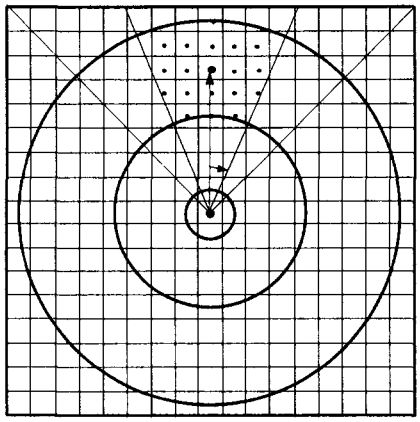

Figure 1. Smoothing fan for sample covariance calculation.

$$\lambda_i = np(i)/dist(i), \qquad \text{with: } \sum_{i=1}^{N} \lambda_i = 1$$

where $np(i)$ is the number of data pairs used to calculate the original experimental covariance value C_i, and $dist(i)$ is the distance between the ith covariance value and the entry $C(k_1, k_2)$ being smoothed.

The window radius $(1 \pm \omega)\rho$ increases with the distance ρ, hence smoothing increases with the lag distance. Indeed, there is usually more unwanted experimental fluctuations at large lags which need to be removed. The parameters ω, $\Delta\theta$, should be chosen such as to include enough data in each smoothing fan.

Since autocovariances are symmetric, $C(\mathbf{h}) = C(-\mathbf{h})$, we need to smooth only half of the covariance map.

FFT and Smoothing of the Spectrum Table

Once the sample covariance table is completed, a *FFT* provides the corresponding pseudodensity spectrum map. Expression (4) considers an equal weighting of all sample covariance values $C(k_1, k_2)$. However, since the reliability of the discrete covariance values $C(k_1, k_2)$ decreases as k_1, k_2 increase, it is appropriate to give more weight to the more reliable smaller lags (k_1, k_2), i.e., consider the weighted expression:

$$\hat{s}(j_1, j_2) = \sum_{k_1=0}^{M_1} \sum_{k_2=0}^{M_2} \lambda_{k_1,k_2} C(k_1, k_2) \exp\left[-2\pi i(k_1 j_1 + k_2 j_2)\right],$$

$$j_1 = 1, \ldots, N_1, \qquad j_2 = 1, \ldots, N_2 \tag{6}$$

where M_1, M_2 are the truncation limits defining the summation window and λ_{k_1,k_2}'s are a set of weights to be applied within that window. Two sets of weights are most frequently used (Chatfield, 1996), corresponding to the

- *Tukey-Hanning window:*

$$\lambda_{k_1,k_2} = \frac{1}{2}\left(1 + \cos \pi \left(\frac{k_1}{M_1} + \frac{k_2}{M_2}\right)\right),$$

$$k_1 = 0, \ldots, M, \qquad k_2 = 0, \ldots, M_2$$

- *Parzen window:*

$$\lambda_{k_1,k_2} = 1 - 6\left(\frac{k_1}{M_1} + \frac{k_2}{M_2}\right)^2 + 6\left(\frac{k_1}{M_1} + \frac{k_2}{M_2 - 2}\right)^3$$

$$0 \le k_1 \le M_1/2, \qquad 0 \le k_2 \le M_2/2$$

$$2\left(1 - \left(\frac{k_1}{M_1} + \frac{k_2}{M_2}\right)\right)^3 \qquad M_1/2 \le k_1 \le M_1,$$

$$M_1/2 \le k_2 \le M/2$$

The above two windows result in similar estimates of the density spectrum values, Chatfield (1991). The window size (values M_1, M_2) is difficult to determine and is obtained by "trial-and-error."

Because density values in expression (4) can be obtained very fast by *FFT*, one can replace the above weighting schemes by a simple moving window average of the type used in expression (5) for the covariance values:

$$\hat{s}(j_1, j_2) = \frac{1}{m_1 m_2} \sum_{l_1 = -m_1/2}^{m_1/2} \sum_{l_2 = -m_2/2}^{m_2/2} s(j_1 + l_1, j_2 + l_2) \tag{7}$$

where m_1, m_2 define a symmetric smoothing window around cell (j_1, j_2).

More precisely, the algorithm proceeds as follows:

- Using *FFT*, transform the gridded sample covariance map into a gridded quasidensity spectrum pdf $s(\mathbf{w})$ using expression (4).
- Smooth $s(\mathbf{w})$ using a moving average of type (7) under constraints of positivity and unit sum to ensure a licit and smoothed spectral pdf.

The constraints for the density spectrum map are:

—spectral density values are real and nonnegative.

—the integral of the density spectrum over the whole range of frequencies w should be equal to $C(0)$, hence if the covariance map has been standardized to a unit variance, then, in $\Re^2$: $\Sigma_{k_1=1}^{N_1} \Sigma_{k_2=1}^{N_2} s(k_1, k_2) = 1$.

—in addition, the smoothed density spectrum should be symmetric about

the zero frequency to ensure that its inverse Fourier transform results in real (nonimaginary) covariance values.

The reason for passing into the spectral domain is the easier positive and bounded condition on the density spectrum, as opposed to checking positive definiteness condition in the spatial (time) domain.

The reason for passing into the spectral domain is the easier positive and bounded condition on the density spectrum, as opposed to checking positive definiteness condition in the spatial (time) domain.

The smoothing window (m_1, m_2) is increased gradually until either the averaged density value (7) becomes nonnegative or the window has reached a predetermined maximum size: in the latter case the entry is assigned a value of 0 to ensure nonnegativity. The extreme case of a zero window size amounts to arbitrarily setting all negative density spectrum values to 0 and then standardizing the whole density map to sum to 1.

Another way to ensure positivity is to "shift" the density spectrum values by a constant value, i.e., $s(\mathbf{w}) = s(\mathbf{w}) - min(0; s(\mathbf{w}), \mathbf{w} \in \Omega), \forall \mathbf{w} \in \Omega$, such that the minimum value of the final density spectrum map is 0. This latter correction works if the largest negative density spectrum value is not too large. Indeed, if $min(0; s(\mathbf{w}), \mathbf{w} \in \Omega)$ is a large value, adding it to the whole spectrum may lead to an almost flat (small variance) spectrum map after standardization to sum 1.

Note: The size (m_1, m_2) of the smoothing window retained may play a critical role on the final results. The fewer the number of original covariance values, the larger the smoothing window, the smoother are the final covariance tables. It is good practice to try a series of smoothing windows with increasing sizes and retain that which gives the covariance table deemed most "realistic," i.e., one that displays the main spatial structures without too much noise. Also, because *FFT* is a global algorithm which accounts for all spectrum values over the whole density map, any outlier in that density spectrum map affects all cells in the transformed covariance table. Therefore, in the sensitivity analysis, one should look at both the density spectrum map and the covariance map.

- The smoothed and licit spectrum $s(\mathbf{w})$ is usable immediately in the frequency domain, e.g., for spectral simulation whether nonconditional (Pardo-Iguzquiza, 1993) or conditional (Yao, 1998), or it can be inversetransformed into a licit covariance lookup table usable, as is, for kriging or conditional simulation in the spatial domain.

Note on Standardization

The most direct way to standardize the spectrum density values to sum up to 1 is through the relation:

$$\hat{s}(j_1, j_2) = \frac{\hat{s}(j_1, j_2)}{\sum_{j_1=1}^{N_1} \sum_{j_2=1}^{N_2} \hat{s}(j_1, j_1)},$$

$$j_1 = 1, \ldots, N_1, \quad j_2 = 1, \ldots, N_2$$

If many original negative density spectrum values have been averaged to a positive value or reset to 0, the sum of all spectrum values is high. Thus, standardization to sum 1 decreases the usually high spectrum density values $s(\mathbf{w})$ found at low frequency components (w small); consequently, the relative impact of these low frequencies on the covariance is decreased, i.e., the covariance is modeled with more high frequencies (nugget effect) than it should. This is not appropriate because the correlation at short lag distance plays the most important role in estimation or simulation and one should not overstate nugget effect. To avoid decreasing the influence of low frequency components, we propose the following standardization expression:

$$\hat{s}(j_1, j_2) = K \cdot \frac{\hat{s}(j_1, j_2)}{\sqrt{j_1^2 + j_2^2}}, \qquad \text{with: } K = 1 \Big/ \sum_{j_1=1}^{N_1} \sum_{j_2=1}^{N_2} \frac{\hat{s}(j_1, j_2)}{\sqrt{j_1^2 + j_2^2}} \tag{8}$$

The original $\hat{s}(\mathbf{w})$ values are corrected proportionally more as $|\mathbf{w}| = \sqrt{(j_1^2 + j_2^2)}$ increases, thus the contribution of the small frequencies (large-scale covariance structures) is least affected.

The Cross-Covariance Case

To ensure positive definiteness of a cokriging matrix without calling for the possibly restrictive linear coregionalization model, one could have considered working in the spatial domain as follows: first build the licit autocovariance lookup tables by the procedure described above, then, smooth the sample cross-covariance in the spatial domain under Schwarz's inequality constraint:

$$|C_{ZY}(h_1, h_2)| \leq \sqrt{C_{ZZ}(h_1, h_2) C_{YY}(h_1, h_2)} \tag{9}$$

However, constraint (9) is neither a sufficient nor a necessary condition for the joint covariance tables to be positive definite. Also, this approach may yield poor fits because the cross-covariance is fit subsequently to the autocovariances. This avenue will not be pursued.

The correct approach is to smooth all auto- and cross-covariances simultaneously in the frequency domain, then inverse transform the auto- and cross-density spectrum maps to get jointly positive definite auto- and cross-covariance lookup tables.

Jointly Smoothing Cross-Spectra

An extension of Bochner's theorem to the multivariate case states that the inverse Fourier transform of a jointly positive definite Hermitian matrix $[s_{kk'}(\mathbf{w})]$ is a jointly positive definite auto- and cross-covariance matrix $[C_{kk'}(\mathbf{h})]$ (Bochner, 1949). For example, in $\Re^2$, the Fourier transform of the cross-covariance $C_{kk'}(\mathbf{h})$ is:

$$s_{kk'}(\omega_1, \omega_2) = \frac{1}{(2\pi)^2} \int_{-\infty}^{+\infty} dh_1 \int_{-\infty}^{+\infty} C_{kk'}(h_1, h_2) \exp\left[i(\omega_1 h_1 + \omega_2 h_2)\right] dh_2$$

The matrix of spectra $\mathbf{s}(\mathbf{w}) = [s_{kk'}(\mathbf{w})]$, $k, k' = 1, \ldots, K$ is said to be Hermitian if:

$$\begin{aligned} s_{kk'}(\omega_1, \omega_2) &= a(\omega_1, \omega_2) + ib(\omega_1, \omega_2) \\ s_{k'k}(\omega_1, \omega_2) &= a(\omega_1, \omega_2) - ib(\omega_1, \omega_2) \end{aligned} \qquad \forall \omega_1, \omega_2 \tag{10}$$

If $\mathbf{s}(\mathbf{w})$ is a Hermitian positive definite matrix for any $\mathbf{w}$, then its inverse Fourier transform $\mathbf{C}(\mathbf{h})$ is a positive definite matrix.

Take the example of two RFs $Z(\mathbf{u})$ and $Y(\mathbf{u})$ in $\Re^2$:

- The Fourier transform matrix $\mathbf{s}(\omega_1, \omega_2)$ of a symmetric cross-covariance, i.e., $C_{k,k'}(\mathbf{h}) = C_{k',k}(\mathbf{h})$, is real-valued and symmetric (Bracewell, 1986). The positive definiteness condition for the real matrix $[s(\omega_1, \omega_2)]$ requires the following determinant to be nonnegative:

$$\begin{vmatrix} s_{ZZ}(\omega_1, \omega_2) & s_{ZY}(\omega_1, \omega_2) \\ s_{ZY}(\omega_1, \omega_2) & s_{YY}(\omega_1, \omega_2) \end{vmatrix}$$

$$= s_{ZZ}(\omega_1, \omega_2) s_{YY}(\omega_1, \omega_2) - [s_{ZY}(\omega_1, \omega_2)]^2 \geq 0, \qquad \forall \omega_1, \omega_2$$

Therefore, smoothing of both auto- and the cross-density spectra can be carried out simultaneously under the constraints:

$$\begin{aligned} &s_{ZZ}(\omega_1, \omega_2) \geq 0, \qquad s_{YY}(\omega_1, \omega_2) \geq 0 \\ &s_{ZY}(\omega_1, \omega_2) \leq \sqrt{s_{ZZ}(\omega_1, \omega_2) s_{YY}(\omega_1, \omega_2)} \end{aligned} \tag{11}$$

The inverse transform of the smoothed result then gives jointly positive definite auto- and cross-covariance lookup tables.

- for an asymmetric cross-covariance:

The Fourier transform matrix $\mathbf{s}(\omega_1, \omega_2)$ is only Hermitian, see definition (10). Then, the positive definiteness constraint of the Hermitian matrix $[s(\omega_1, \omega_2)]$ requires the following determinant to be nonnegative:

$$\begin{vmatrix} s_{ZZ}(\omega_1, \omega_2) & s_{ZY}(\omega_1, \omega_2) \\ s_{YZ}(\omega_1, \omega_2) & s_{YY}(\omega_1, \omega_2) \end{vmatrix}$$

$$= \begin{vmatrix} s_{ZZ}(\omega_1, \omega_2) & a(\omega_1, \omega_2) + ib(\omega_1, \omega_2) \\ a(\omega_1, \omega_2) - ib(\omega_1, \omega_2) & s_{YY}(\omega_1, \omega_2) \end{vmatrix}$$

$$= s_{ZZ}(\omega_1, \omega_2)s_{YY}(\omega_1, \omega_2) - [a^2(\omega_1, \omega_2) + b^2(\omega_1, \omega_2)] \geq 0, \qquad \forall \omega_1, \omega_2$$

therefore, both auto- and cross-density spectra can be smoothed simultaneously under the constraints:

$$\begin{aligned} & s_{ZZ}(\omega_1, \omega_2) \geq 0.0, \qquad s_{YY}(\omega_1, \omega_2) \geq 0.0 \\ & a^2(\omega_1, \omega_2) + b^2(\omega_1, \omega_2) \leq s_{ZZ}(\omega_1, \omega_2)s_{YY}(\omega_1, \omega_2) \end{aligned} \qquad \forall \omega_1, \omega_2 \quad (12)$$

The inverse Fourier transform then gives jointly positive definite covariance lookup tables for the autocovariances C_Z, C_Y and the asymmetric cross-covariance C_{ZY}, C_{YZ}.

The joint smoothing of spectrum maps calls for moving averages similar to those used for autospectrum smoothing, with in addition the stricter last constraint (12). The smoothing window (values m_1, m_2) as used in expression (7) is increased gradually until these conditions are met or until the window has reached a predetermined maximum size. In the latter case,

- if the autodensity spectrum values are still negative, they are arbitrarily set to 0:
- if the last inequality (12) is still not respected, a correction proportion p is applied on the coefficients $a(\omega_1, \omega_2)$, $b(\omega_1, \omega_2)$ to satisfy it:

$$(a(\omega_1, \omega_2) \cdot p)^2 + (b(\omega_1, \omega_2) \cdot p)^2 = s_{ZZ}(\omega_1, \omega_2) \cdot s_{YY}(\omega_1, \omega_2)$$

that is:

$$p = \sqrt{s_{ZZ}(\omega_1, \omega_2) \cdot s_{YY}(\omega_1, \omega_2)/(a(\omega_1, \omega_2)^2 + b(\omega_1, \omega_2)^2)}$$

then set:

$$a(\omega_1, \omega_2) = a(\omega_1, \omega_2) \cdot p$$

$$b(\omega_1, \omega_2) = b(\omega_1, \omega_2) \cdot p$$

A straightforward inverse *FFT* will provide jointly positive definite (cross) covariance tables.

Using the Covariance Lookup Table

By direct reading from a licit covariance lookup table, kriging systems can be built without calling for any specific close-form analytical covariance model. All traditional estimation and simulation programs can be modified to read directly from such covariance lookup table. The parameters for the covariance/variogram model in the parameter files for the estimation and simulation programs in *GSLIB* (Deutsch and Journel, 1992), can be replaced by an input data file containing the licit covariance map in 2-D or cube in 3-D.

Note. Even in 3-D, the file containing a covariance cube is not likely to be very large because, in practice, the data used in kriging/cokriging are limited to a neighborhood centered on the point being estimated, hence the maximum distance $\mathbf{h}$ to be included in the covariance cube is correspondingly limited. A more critical problem is that of the usually dense grids of simulation calling for equally dense (hence large in size) covariance cubes, but then one could approximate an unavailable covariance value $C(\mathbf{h})$ by the entry available $C(\mathbf{h}')$ with $\mathbf{h}'$ closest to $\mathbf{h}$.

CASE STUDY

For the case study, we use a standardized correlogram rather than a covariance and all developments are carried out in the normal score space. Therefore, the random function modeling the primary variable U has a unit variance. The normal scores of the 140 data of the *GSLIB* data file **cluster.dat** are used as conditioning data (Deutsch & Journel, 1992, p. 37). The reference images of both the primary variable U and the secondary variable V are shown in the upper row of Figure 2, followed by the location maps of the 140 clustered conditioning samples and their statistics. The exhaustive map of the secondary variable V displays spatial structures similar to those of the primary variable U, although with smaller variance because V is actually a moving spatial average of original 3-D U-values.

Sample and Exhaustive Correlogram Maps

First, the autocorrelogram and cross-correlogram maps, each of dimension 65×65 for the two variables U and V, are calculated from the 140 sample data; they are displayed in Figure 3. The dimension 65 larger than the field dimension 50 is needed for implementation of the fast Fourier transform. Due to the small number of data pairs available for calculation in each cell, the sample correlogram map shows a lot of fluctuations and also many missing entries (white pixels in Fig. 3). The extent of these fluctuations is better appre-

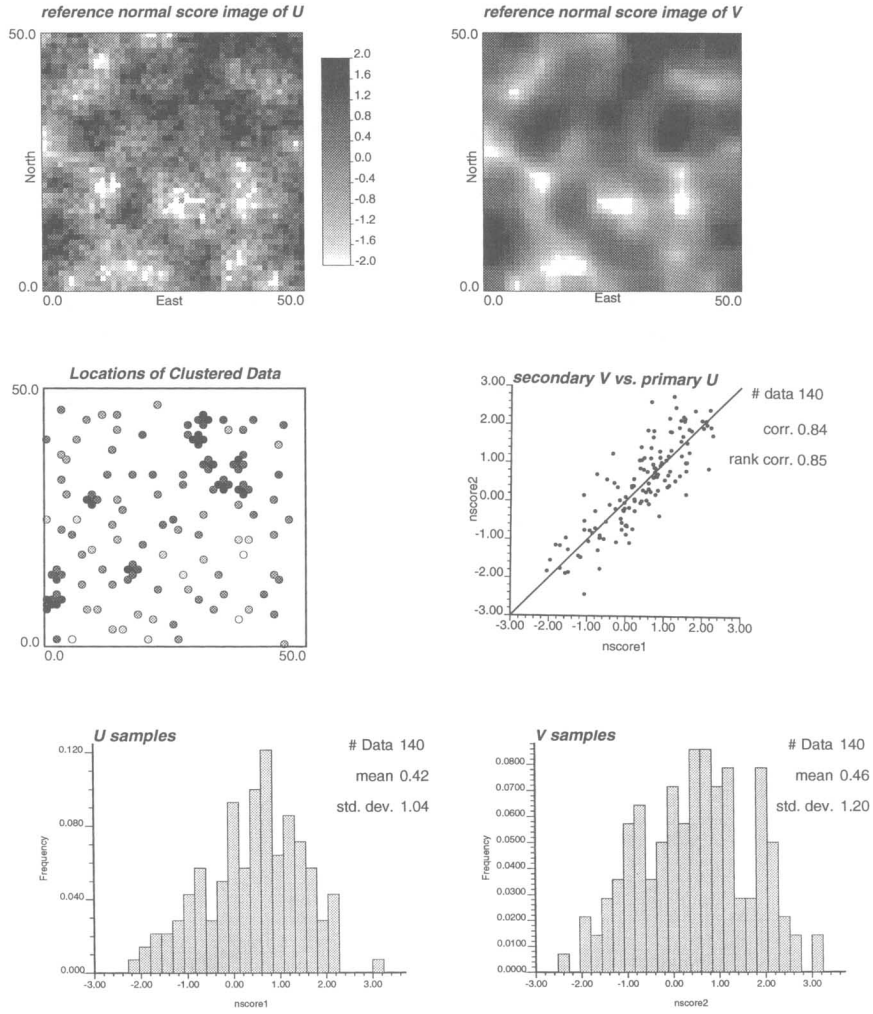

Figure 2. Reference images and sample location maps of U, V, and their statistics.

ciated in Figure 4 which displays four section views of the correlogram map of U along four directions. For comparison, we also calculated the pseudocorrelogram maps from the 2500 exhaustive data and retrieve the same four directional U-correlograms (see Figs. 5 and 6). The neat spatial structures reflected by the exhaustive reference data are poorly captured by the 140 sample cor-

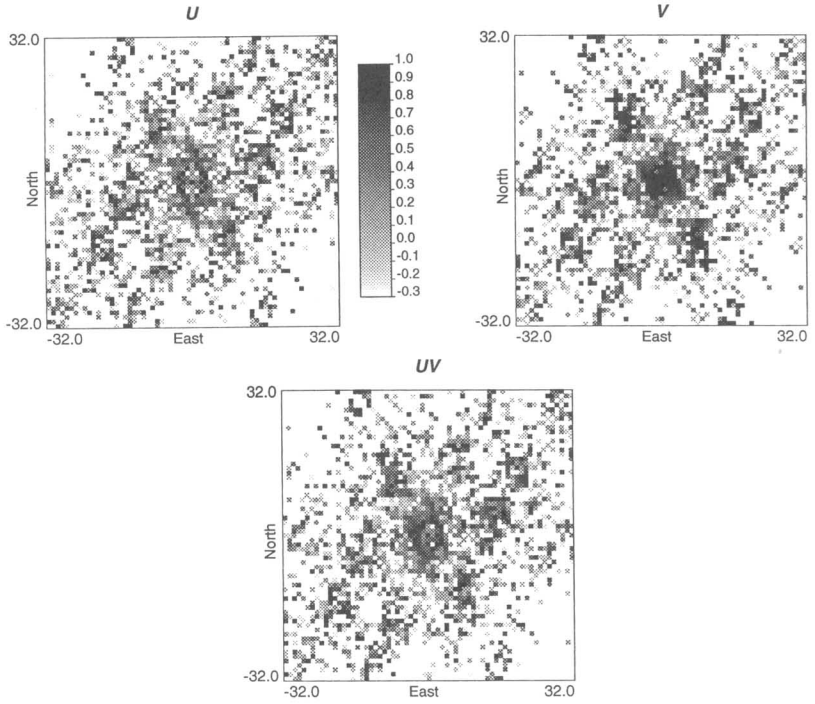

Figure 3. Sample (cross) correlogram maps of U and V, calculated from 140 clustered data.

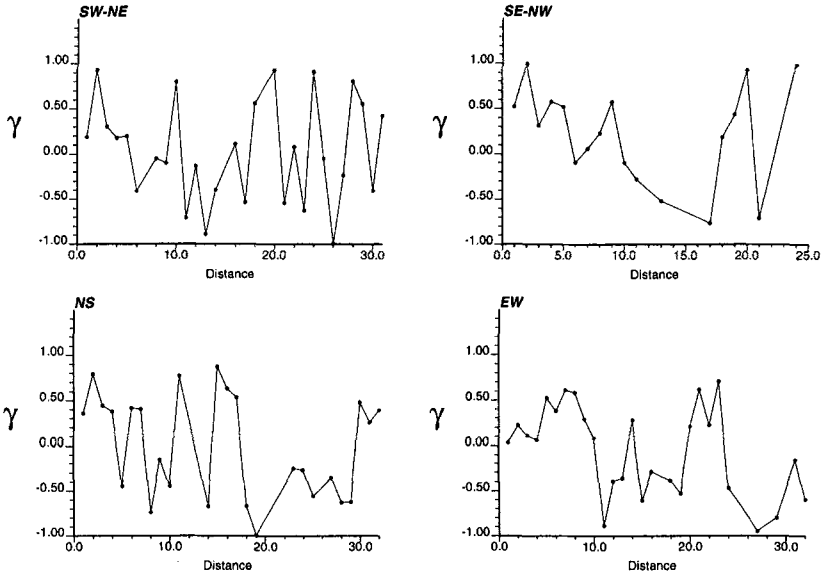

Figure 4. Sample correlogram of U in directions SW–NE, SE–NW, NS, and EW.

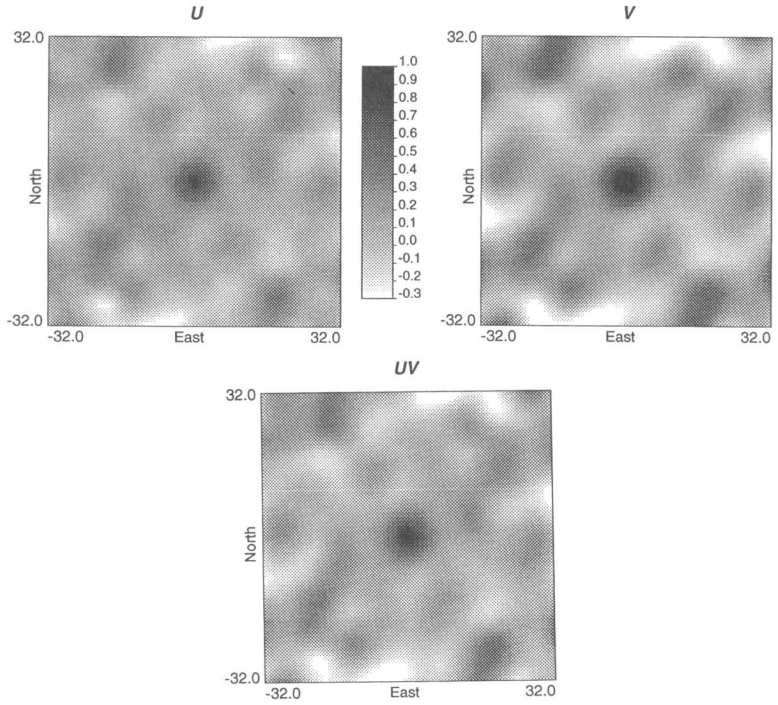

Figure 5. (Cross) correlogram maps of U and V, calculated from the 2500 exhaustive data.

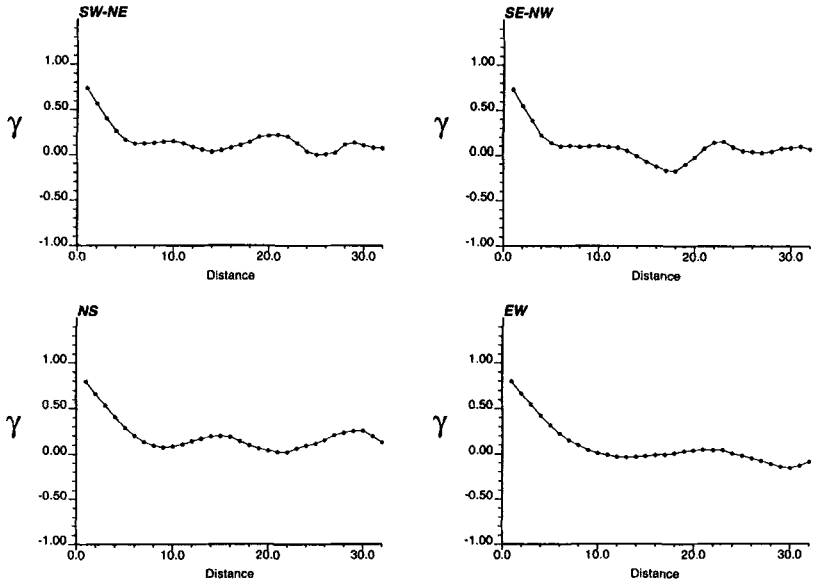

Figure 6. Exhaustive correlogram of U in four directions.

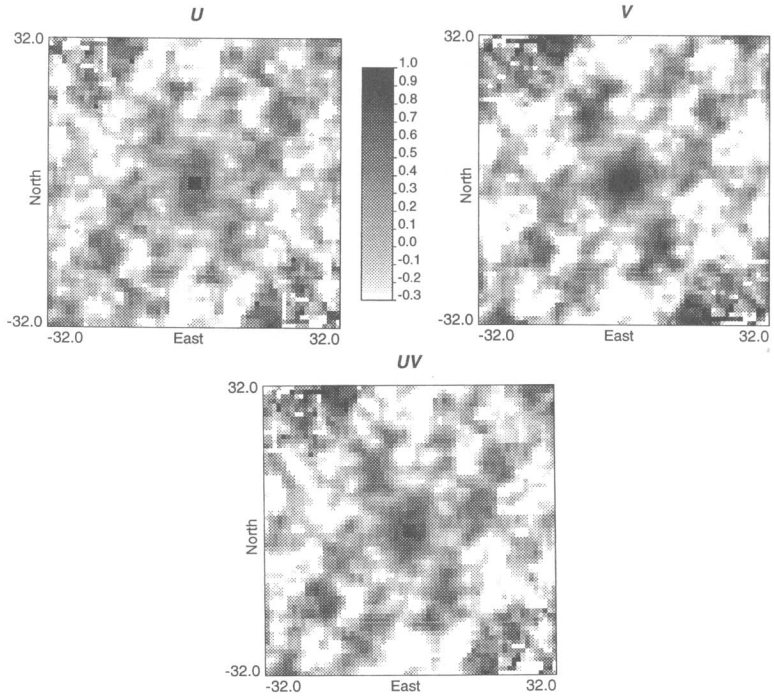

Figure 7. Sample (cross) correlogram maps of U and V, calculated from 140 clustered data, allowing for tolerance.

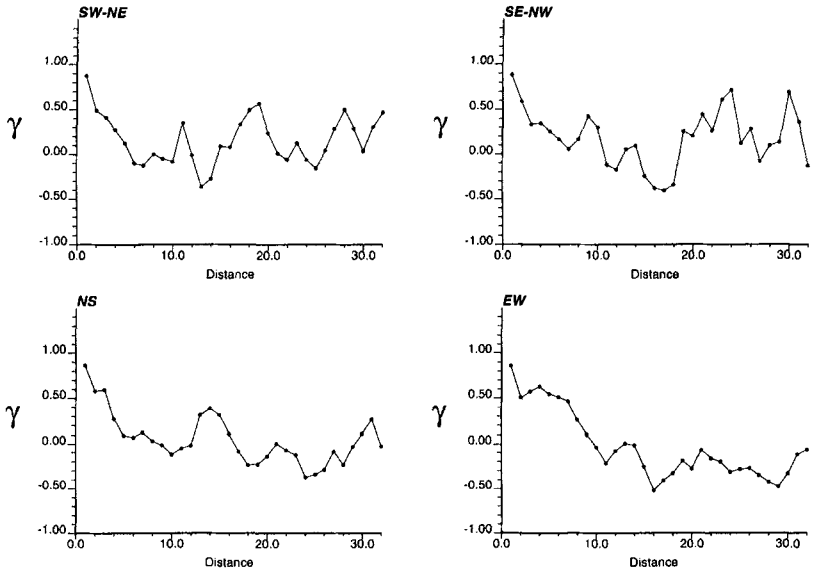

Figure 8. Sample correlogram of U in four directions, allowing for tolerance.

relogram maps. To improve the sample correlogram map, we applied a tolerance of (1, 1) on the calculation. That is, a data pair occurring in a cell (i, j) also contributes to all cells within its neighborhood $(i', j') \in \{i \pm 1, j \pm 1\}$. In this way, more data pairs are used for the calculation of each cell in the correlogram map: this results in the smoother and more accurate correlogram maps shown in Figures 7 and 8. Note that there are still a few missing entries at the border of the maps of Figure 7.

Automatic Modeling of Correlogram Maps

Starting from the experimental auto- and cross-correlogram maps in Figure 7, we carried out an initial interpolation and smoothing to fill in the missing entries and remove some of the sample fluctuations; the resulting images are shown in Figures 9 and 10 to be compared with Figures 3 and 4. The starting radius of the smoothing fan was $[(1 - 0.1)\rho, (1 + 0.1)\rho]$. If there is less than the preset minimal 4 data within the fan, the fan is enlarged by a 0.01ρ increment each time, until the minimum number of 4 data is reached. The starting radius, the radius increment and the preset minimum number of data are parameters that can be adjusted by the user.

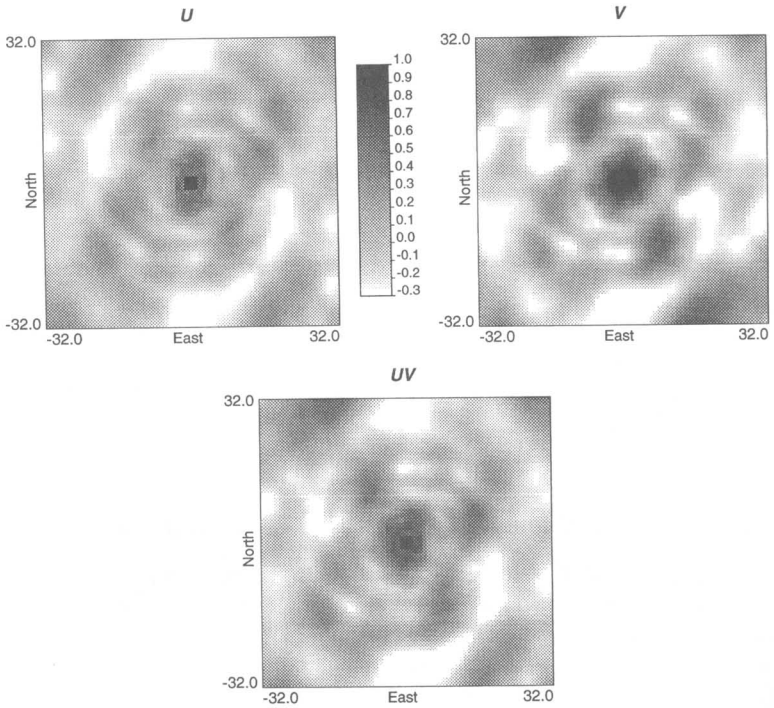

Figure 9. Sample (cross) correlogram maps of U and V after interpolation.

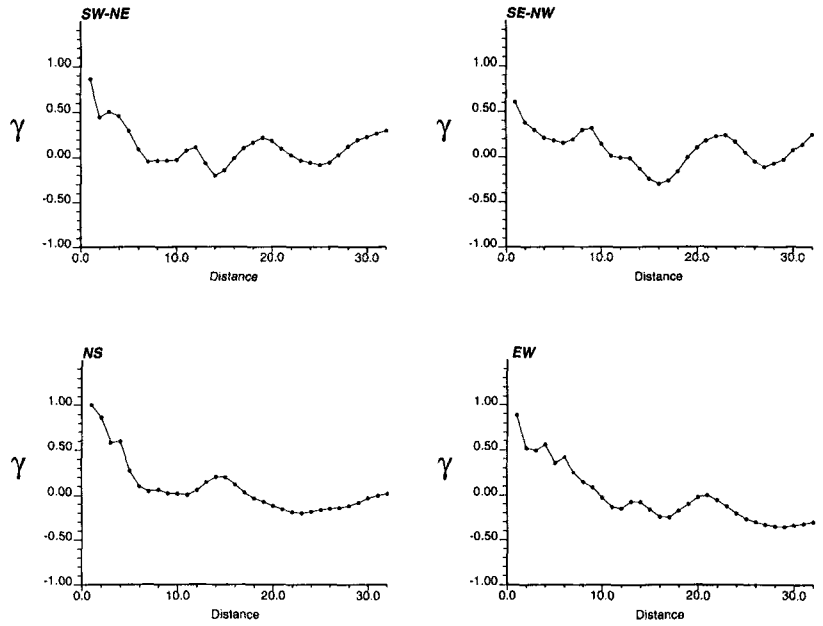

Figure 10. Sample correlogram of U in four directions, after interpolation.

Once the correlogram maps are filled in, *FFT* is carried out to get the sample pseudodensity spectrum maps, which are then smoothed under the constraints (12). Figure 11 shows the inverse-transformed correlogram maps using a smoothing window size 7×7. The four section views of the final smoothed U correlogram map using the 7×7 smoothing window are shown in Figure 12; they are plotted next to the corresponding sections from the reference U correlogram map. Note the excellent and smoothed fit of the reference correlograms as compared to the original sample fluctuations of Figure 4. The proposed *FFT* "roundtrip" has not only ensured positive definiteness of the final correlogram map but has also filtered out most of the experimental fluctuations associated to data sparsity. Figures 13 and 14 give the corresponding results for the V-correlogram and U-V cross-correlogram.

Estimation and Simulation Using the Final Correlogram Tables

Using the final smoothed correlogram maps, kriging can proceed. For comparison purposes, we performed kriging reading the correlogram values from the final correlogram maps of Figure 11 and, by reading from the analytical linear coregionalization model given in Deutsch and Journel (1992, p. 250), i.e.,

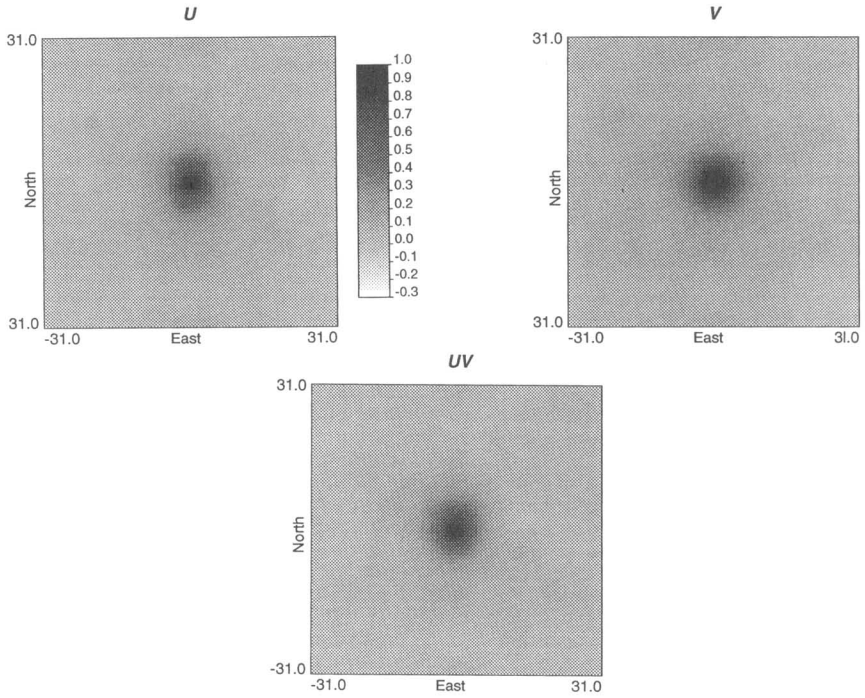

Figure 11. Smoothed jointly positive definite (cross) correlogram maps, with a 7 × 7 smoothing window in frequency domain.

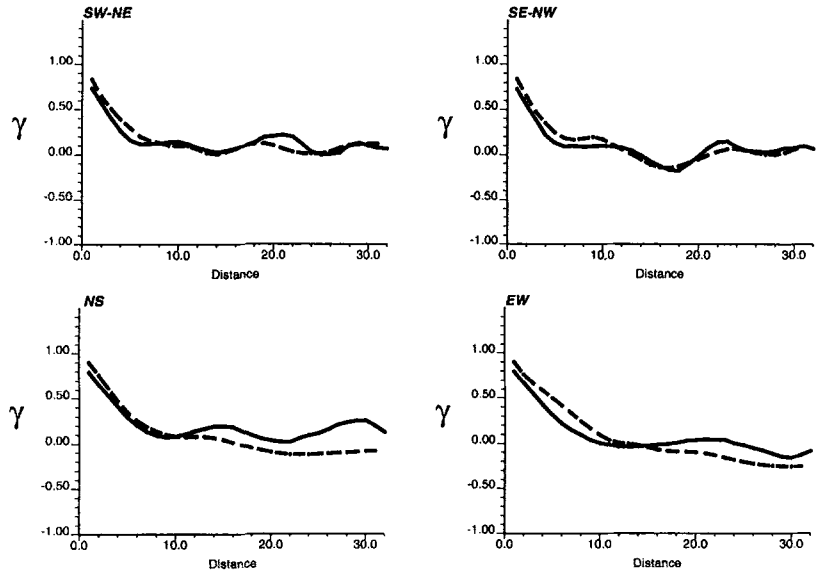

Figure 12. Final smoothed correlogram of U in four directions (---), compared with the reference (——).

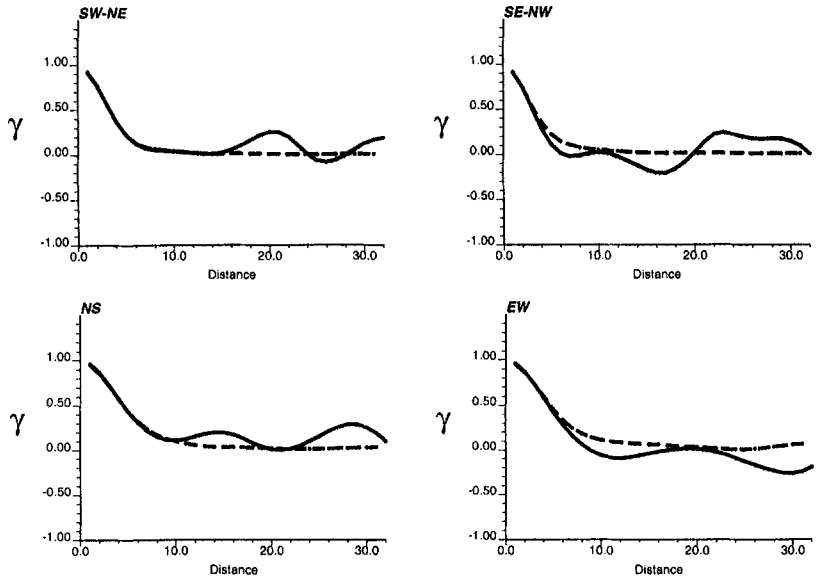

Figure 13. Final smoothed correlogram of V in four directions (---), compared with the reference (——).

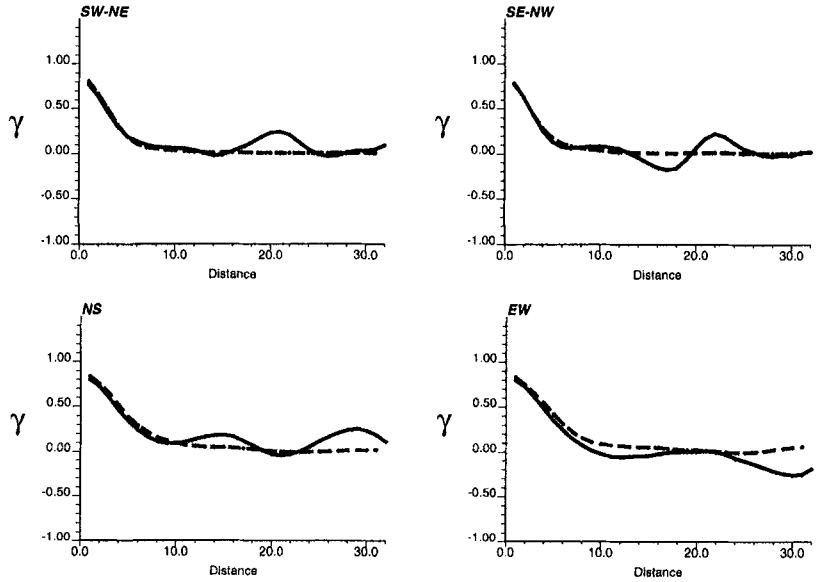

Figure 14. Final smoothed cross correlogram of U-V in four directions (---), compared with the reference (——).

$$\begin{cases} \gamma_U(\mathbf{h}) = 0.238 + 0.762\,Sph(|\mathbf{h}|)/10) \\ \gamma_V(\mathbf{h}) = 0.005 + 0.995\,Sph(|\mathbf{h}|)/10) \\ \gamma_{UV}(\mathbf{h}) = 0.0 + 0.649\,Sph(|\mathbf{h}|)/10) \end{cases} \tag{13}$$

where $Sph(\mathbf{h}|/a)$ represent a spherical structure of range a.

The correlogram maps corresponding to that analytical model are shown in Figure 15, to be compared to the exhaustive pseudocovariance maps of Figure 6. Note the (common) underestimation of the correlation values for small lags **h**.

Because that the coregionalization model (13) and Figure 15 were obtained from the exhaustive data. Conversely, the covariance table of Figure 11 was built from only the 140 collocated samples of U and V. Yet this later table reflects better the critical high correlation values for small lags **h**.

The location map of the U samples and the U reference image are shown on Figure 2. The kriging estimates reading from the analytical traditional variogram model (13), then from the smoothed correlogram map of Figure 11 are compared in Figure 16; the corresponding two scatterplots between estimated

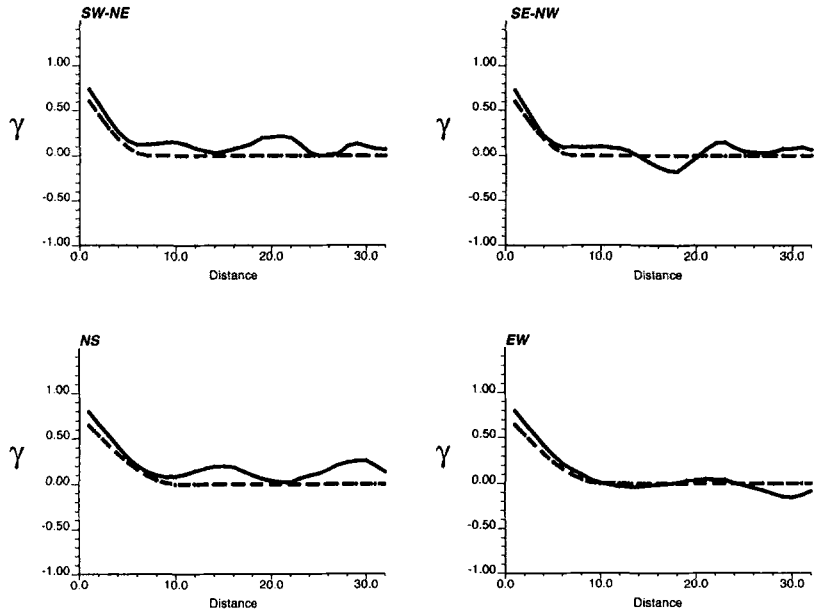

Figure 15. Correlogram of U in four directions built from the analytical variogram model (---), compared with reference (——).

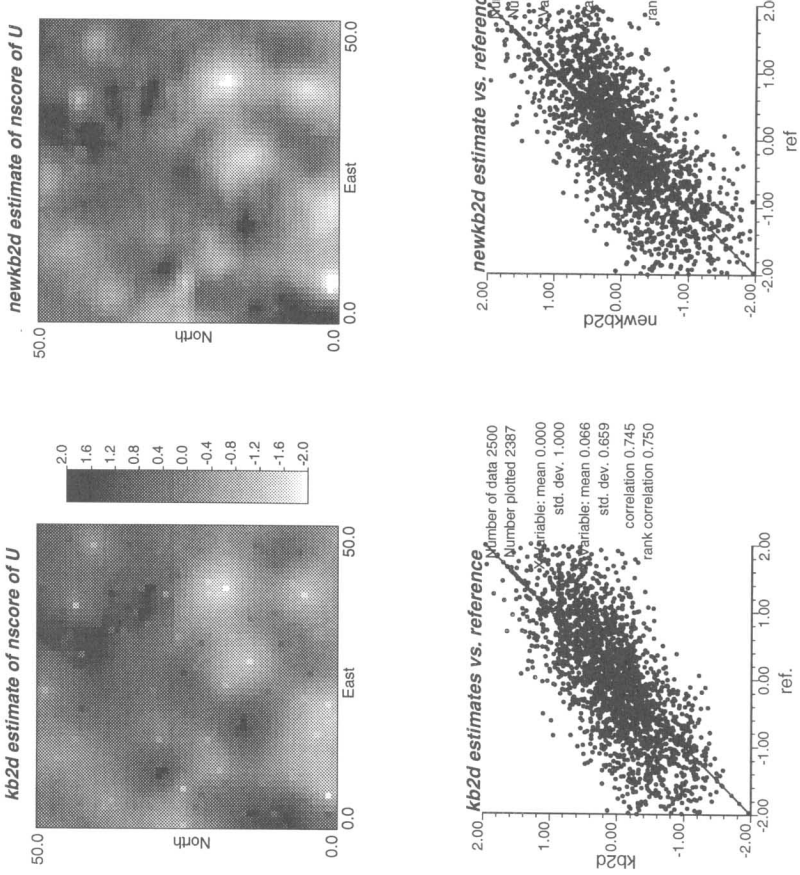

Figure 16. Comparing kriging estimates of U using the traditional modeling approach and reading from the automatically-derived correlogram table.

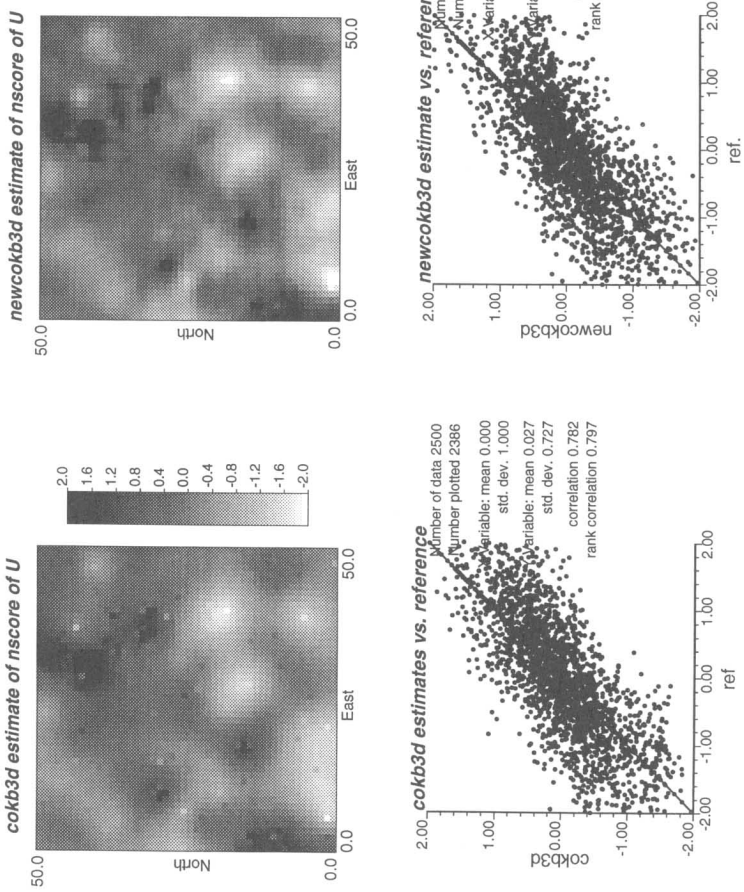

Figure 17. Comparing cokriging estimates of U using the traditional linear coregionalization model and reading from the (cross) correlogram tables. Only collocated secondary data are used.

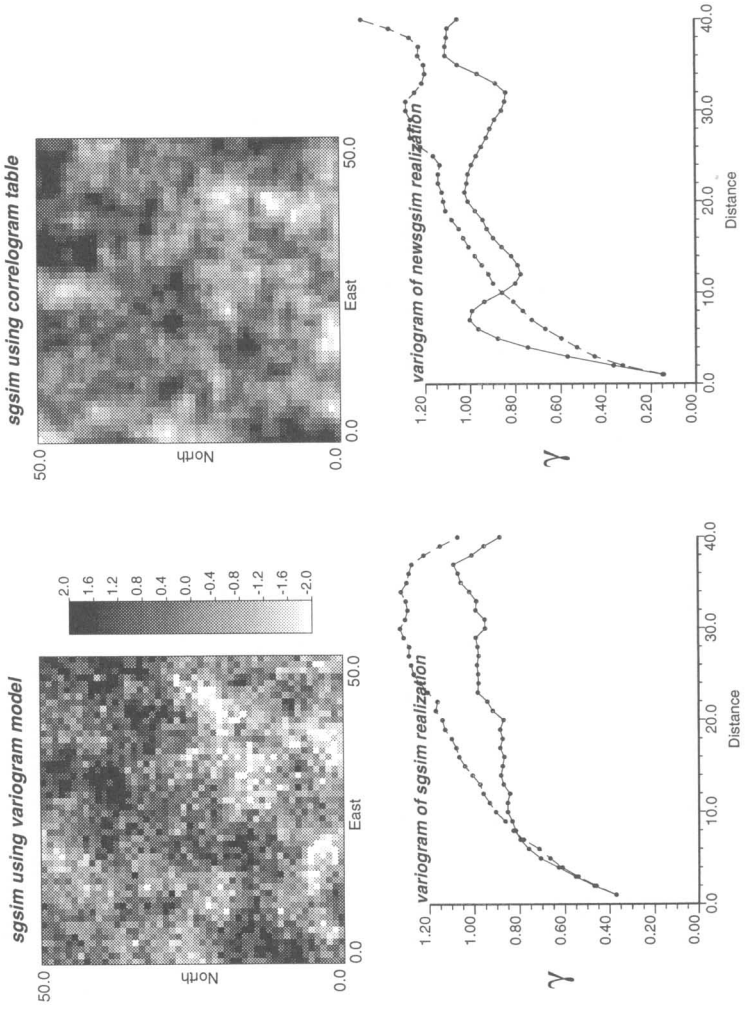
sgsim using correlogram table
sgsim using variogram model
variogram of newsgsim realization
variogram of sgsim realization
North
East
Distance
γ
50.0
0.0
2.0
1.6
1.2
0.8
0.4
0.0
-0.4
-0.8
-1.2
-1.6
-2.0
1.20
1.00
0.80
0.60
0.40
0.20
0.00
10.0
20.0
30.0
40.0

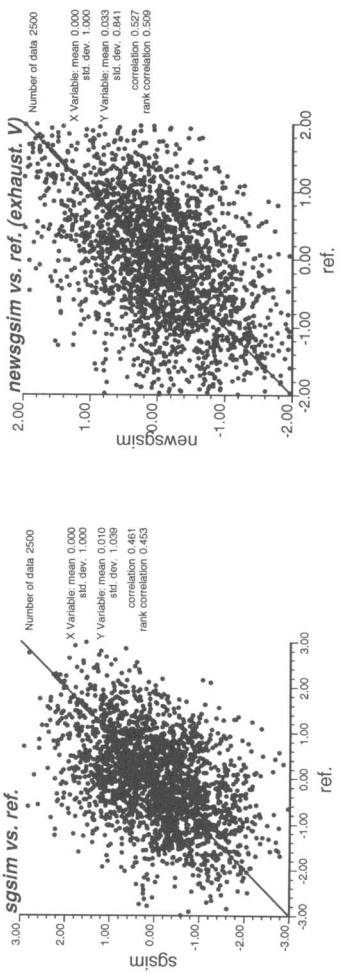

Figure 18. Comparing sgsim realizations of U using the traditional modeling approach and reading from the correlogram table: simulated variograms and scatterplots of simulated reference values.

values and reference data are also given. The two sets of kriging estimates appear quite similar: the map obtained by reading from the correlogram table (**newkb2d**) appears less smooth.

Similarly, we used both the analytical model (13) and the (cross) correlograms table of Figure 11 to perform a cokriging estimation. The results are shown in Figure 17. For cokriging, we used only the V-data collocated with the value U being estimated. Again, the results from the two different covariance readings are very similar.

Reading from permissible correlogram tables, conditional simulation can also be carried out in the spatial domain. Fifty simulated realizations were drawn using the sequential Gaussian algorithm, using both the traditional variogram model and reading from the correlogram table of Figure 11. The two first realizations are shown in Figure 18, with the simulated variograms in NS and EW directions. The simulated results using the correlogram table displays less fluctuations: this is explained by the smaller nugget implicit to the correlogram table of Figure 11.

CONCLUSIONS

- The proposed new approach for automatic covariance modeling consists of transforming the experimental (cross) covariance tables into spectral density tables in the frequency domain using *FFT*. Following Bochner's theorem, the spectral density maps are smoothed in this frequency domain under proper positivity constraints. The *FFT* inversetransform of the smoothed spectral density tables provides (jointly) positive definite (cross) covariance tables.
- The transformation between spatial and frequency domain can be done very fast using *FFT*. The constraints for positive definiteness in the frequency domain are easy to implement. The main advantage of the technique is that it does not call for any prior choice of an analytical model, and frees the modeling of coregionalization from the restriction of the linear coregionalization model and the burden of its fit.
- The intermediary smoothed density spectrum map can be used directly for spectral simulation in the frequency domain. Its *FFT* inversetransform yields permissible (cross) covariance maps from which the necessary covariance values can be read directly for either kriging or stochastic simulation.
- The preliminary case study developed indicates that the proposed automatic covariance map determination is much faster and easier to implement than traditional analytical covariance/variogram modeling, yet yields comparable if not better results for kriging and simulation.

REFERENCES

Almeida, A., and Journel, A., 1994, Joint simulation of multiple variables with a Markov-type coregionalization model: Math. Geology, v. 26, no. 10, p. 565–588.

Bochner, S., 1949, Fourier transform: Princeton Univ. Press, London, 219 p.

Bracewell, R., 1986, The Fourier transform and its application: Mc-Graw Hill, Singapore, 474 p.

Chatfield, C., 1996, The analysis of time series: an introduction: Chapman & Hall Ltd., London, 283 p.

Chu, J., 1993, Conditional fractal simulation, sequential indicator simulation, and interactive variogram modeling: unpubl. Doctoral dissertation, Stanford University, 147 p.

Deutsch, C., and Journel, A., 1997, Geostatistical software library and user's guide: Oxford Univ. Press, New York, 368 p.

Deutsch, C., 1996, Direct assessment of accuracy and precision, *in* Baffi, E., and Schofield, N., eds., Geostatistics Wollongong '96 (Vol. 1): Kluwer Academic Publ., Dordrecht, p. 115–125.

Goulard, M., 1989, Inference in a coregionalized model, *in* Armstrong, M., ed., Geostatistics (Vol. 1): Kluwer Academic Publ., Dordrecht, p. 397–408.

Journel, A., and Huijbregts, C., 1978, Mining geostatistics: Academic Press, San Diego, 600 p.

Journel, A., 1996, Deterministic geostatistics: A new visit, *in* Baffi, E., and Schofield, N., eds., Geostatistics Wollongong '96 (Vol. 1): Kluwer Academic Publ., Dordhrect, p. 174–187.

Pardo-Iguzquiza, E., and Chica-Olmo, M., 1993, The Fourier integral method: An efficient spectral method for simulation of random fields: Math. Geology, v. 25, no. 4, p. 177–217.

Rehman, S., 1995, Semiparametric modeling of cross-semiovariograms: unpubl. Doctoral dissertation, Georgia Institute of Technology, 143 p.

Sneddon, L., 1951, Fourier transforms: McGraw Hill, New York, 542 p.

Yao, T., Conditional spectral simulation with phase identification: Math. Geology, v. 30, no. 3, p. 285–308.